Pharmaceutical Research, Vol. 22, No. 8, August 2005 (© 2005)
DOI: 10.1007/s11095-005-5280-x

Research Paper

Location-Dependent Analysis of Porosity and Pore Direction in Tablets

Yu San Wu,[1,5] Henderik W. Frijlink,[1] Lucas J. van Vliet,[2] Ietse Stokroos,[3] and Kees van der Voort Maarschalk[1,4]

Received February 9, 2005; accepted March 22, 2005

Purpose. Several phenomena in tablets indicate that an inhomogeneous pore distribution is formed during the compaction process. Examples are lamination and the capping of corners. In order to gain an understanding of the relation between structure and compact properties, analyzing the structure in a location dependent manner would be extremely useful. Our aim was to visualize and to quantitatively analyze the pore distribution in compacts.
Methods. This was done by embedding a cubic (sodium chloride) compact with polymer, allowing the compact to be cut without disrupting the structure. By doing so, it was possible to make scanning electron microscopic images from different angles at different locations in the compact. These images were made binary with a two-means cluster algorithm (Isodata) after which the porosity could be calculated. Counting the number of transitions from the pixels in the pores to the pixels in the sodium chloride particles in two perpendicular directions allows us to construct a measure for the anisotropic connectivity of the particles.
Results. The results show an increase in porosity toward the bottom of the compact and showed a preferred orientation of the pores in the direction of compression.
Conclusions. The proposed method is suitable for analyzing the pore distribution quantitatively and for evaluating anisotropy.

KEY WORDS: anisotropy; compaction; imaging; pore characterization; pore structure.

INTRODUCTION

Despite the popularity of tablets as a dosage form, problems during tabletting and with the produced tablets occur frequently. Because failures such as lamination and the capping of corners occur in specific locations of the tablet, inhomogeneity in (pore) structure is expected.

Inhomogeneity in structure cannot be evaluated with the current methods such as mercury porosimetry and gas adsorption. These methods consider the compact as a whole and discard important local variations. For a better understanding of compact properties, analyzing structure as a function of location within a compact is quite useful.

An important parameter describing the structure is the pore network in a compact. Ryshkwitch described the relationship between bulk porosity and tensile strength, stating that there is a linear relation between the bulk porosity and the logarithm of the tensile strength (1). However, this does not explain all differences in tensile strength. It has been hypothesised that the pore shape also has an important influence on tensile strength (2,3). Thus, it is desirable to characterize the pore distribution on a smaller scale than an entire compact. One factor that could then be evaluated is the anisotropy, meaning that a property is dependent on the direction in which it is measured. Anisotropy in structure is suggested by anisotropy in tensile strength, as reported by several authors (4–7). Ando *et al.* (4) made pictures of cross sections of the tablets revealing anisotropy in structure, but no quantitative information was obtained (4).

Obtaining detailed information about pore distribution is difficult. Current methods have the disadvantage that they measure only porosity and pore size distribution of an entire compact; no information about the shape or the direction of the pores is obtained. Modern techniques such as X-ray computed tomography enable visualization of the pore morphology as demonstrated in granules (8,9), but the current resolution of this method (approximately 10 μm) is not sufficient, yet, for the evaluation of pore distribution (shape) in compacts, as the pore diameter is typically in the order of 1 μm or even less (10–12).

To gain a fundamental understanding of compact properties in relation to pore distribution, a more detailed

[1] Department of Pharmaceutical Technology and Biopharmacy, Groningen University Institute for Drug Exploration (GUIDE), Ant. Deusinglaan 1, 9713 AV Groningen, The Netherlands.
[2] Quantitative Imaging Group, Department of Imaging Science & Technology, Faculty of Applied Sciences, Delft University of Technology, Delft, The Netherlands.
[3] Laboratory for Cell Biology and Electron Microscopy, University of Groningen, Groningen, The Netherlands.
[4] Department of Pharmaceutics, NV Organon, Oss, The Netherlands.
[5] To whom correspondence should be addressed. (e-mail: y.s.wu@rug.nl)

ABBREVIATIONS: GMA, glycol methacrylate; SEM, scanning electron microscope.

characterization is needed. The development of a suitable method for this purpose forms the aim of the research described in this article. The method presented here describes how pore distribution can be visualized and quantitatively analyzed.

MATERIALS AND METHODS

Experimental Setup

To investigate the pore distribution in the compact, different planes in a cubic sodium chloride tablet of $7 \times 7 \times 7$ mm were analyzed. The tablets were made with uniaxial compression. A cube has the advantage that the dimensions of the tablet are the same irrespective of the direction of testing, thus making it easier to examine the tablet structure, for instance the anisotropy, and to check the validity of the imaging method. We examined the structure by making plan and elevation photos.

Plan photos provide a top view and are made when looking down on the tablet at different heights, in the same direction as compression was performed. This direction is defined as the z-direction. Plan photos were made of different planes in the tablets (Fig. 1A). The first plane is the upper surface of the cube. The other planes lie parallel to this plane at 1.75 mm, 3.5 mm, and 5.25 mm from the upper surface. These distances were arbitrarily chosen, but at equal distance from each other. In the plan photos, an x- and a y-direction were defined. Both directions lie parallel to the cube axes.

Elevation photos provide a side view, observed from the compression direction, of the tablet structure. These photos

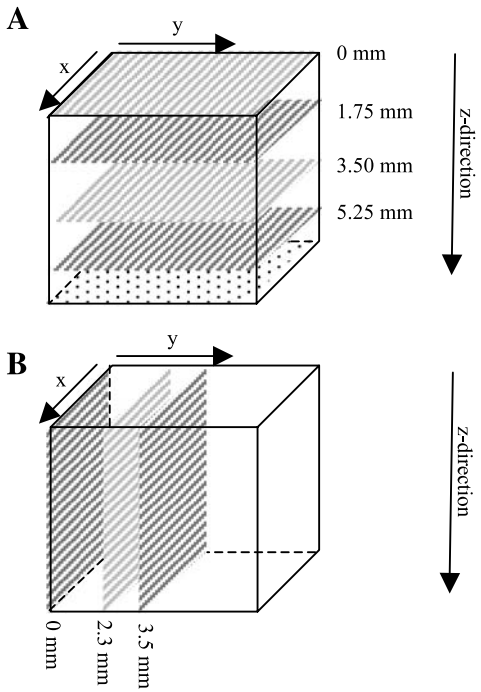

Fig. 1. (A) The different planes in the compact of which plan photos are made. (B) The different planes in the compact of which elevation photos are made.

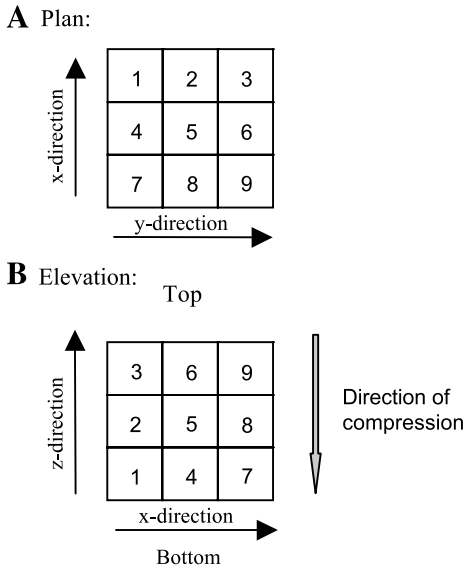

Fig. 2. (A) Photo positions of the plan photos. (B) Photo positions of the elevation photos.

were made of three different planes. The first plane is a randomly chosen side plane of the cube. The other planes lie parallel to this plane at 2.3 mm and 3.5 mm from the side (see Fig. 1B). Only one half of the tablet was examined as plane symmetry was expected. In each of these planes an x- and z-direction are defined.

Of each plane 9 photos were taken. These images almost cover the whole plane. Figure 2A depicts which photo number corresponds to which position for the plan photos. Photo position 5 corresponds to the center of the plane, while photos 1, 3, 7, and 9 correspond to the corner positions. For the elevation photos, 1, 4, and 7 are closest to the bottom of the tablet, while 3, 6, and 9 are closest to the top of the tablet as shown in Fig. 2B.

EXPERIMENTAL METHODS

Materials

The 212–250 μm fraction of sodium chloride (chemically pure quality, Akzo Nobel, Hengelo, The Netherlands) was obtained by 30 min vibratory sieving (Fritsch analysette 3, Germany) followed by 12 min air jet sieving over a sieve of 212 μm (Alpine A200, Augsburg, Germany) to remove the fines. The true density of the 212–250 μm fraction as measured with helium pycnometry (Quantachrome, Syosset, New York, USA) was 2175 kg/m^3.

Tablet Compaction

A specially manufactured die was used to compress the compacts. The die was square shaped, both sides being 7 mm. Before compaction, the die was lubricated with magnesium stearate using a brush. After the die was filled with 530 mg of sodium chloride, the powder was compacted with 2.25 kN using a hydraulic press (ESH compaction apparatus, Hydro Mooi, Appingedam, The Netherlands). The rate of compac-

tion was 0.5 kN/s and the maximum pressure was maintained for 0.1 s. Compact dimensions were measured after 24 h with an electronic micrometer (Mitutoyo, Tokyo, Japan) and the weight of the compacts was measured with an analytical balance (Mettler-Toledo, Greifensee, Switzerland). From these data and the real density the final porosity was calculated. The target porosity of the tablets was 30%. The standard deviation of the porosities of all tablets was 0.3%. This porosity was chosen because it still resulted in manageable tablets with a high porosity, ensuring that the tablet could be completely infiltrated with polymer.

Embedding and Cutting the Slices

Compacts were embedded in glycol methacrylate (GMA). This technique is widely used for embedding of biological specimens and subsequent sectioning. A desired volume of Technovit 7100 (Kulzer, Germany) was carefully mixed with hardener I. Shortly before embedding the compact, a second hardener was added. The compacts were immersed with the mixture and completely infiltrated and subsequently stored at room temperature for 2 days.

To make photos of the designated planes in the compact, the appropriate quantity of sodium chloride/polymer matrix was scraped off of the sample with a lathe (Schaublin 125, Esmeijer, Rotterdam, The Netherlands). After scraping off the material with the lathe, a microtome (Reichert-Jung 2050, Vienna, Austria) was used to slice off approximately 1 μm material to obtain a smooth surface. These surfaces were used for scanning electron microscopic (SEM) inspection.

Images

The images were made using back scattered electron imaging. With this technique, also used by Sriamornsk (13), a good contrast is achieved between regions with sodium chloride and regions where the polymer is present. The reason is that elements with a higher atomic number (i.e., the sodium and chloride in our case) deflect more electrons than elements with a lower atomic number (i.e., the polymer). Therefore the elements with a lower atomic number are represented by the darker regions in the image.

SEMs were made using a JEOL scanning electron microscope (JEOL, type JSM-6301F, Japan) operated at an accelerating voltage of 10 kV. The diaphragm was 50 μm, spot size 6, and the working distance was 15 mm. Back scatter was used (standard backscatter detector, JEOL, Japan). Samples were not coated and the magnification was 60×.

IMAGE ANALYSIS

Local Porosity

Each picture used for calculation of the local porosity had a size of 1676 × 1676 pixels. Matlab 6.5.1 (The MathWorks Inc, Natick, USA) and the Dipimage toolbox (Quantitative Imaging Group, Faculty of Applied Sciences, Delft University of Technology, the Netherlands) (14) were used for the image analysis. With this software, the gray-scale images were made binary with the Isodata threshold algorithm (15). This algorithm calculates the best threshold value out of the gray value histogram of the image.

The binary images consist of two phases. One phase, "salt phase," corresponds to the surface area containing the sodium chloride particles. The other phase, the "pore phase," corresponds to the places where the polymer had replaced the air in the original pores in the compact. In each binary image the total number of pixels in the pore phase was counted. With this number the local porosity was calculated:

$$\varepsilon_l = \frac{N_{pixel\_pore}}{N_{pixel\_image}} \times 100\%$$

in which:

ε_l = local porosity in percentage
N_{pixel_pore} = number of pixels in the pore phase
N_{pixel_image} = number of pixels in the image

The plan photos at a tablet depth of 1.75 mm were made without using the microtome first. Therefore, the calculated local porosities of these images were corrected by adding the mean difference between the local porosity before and after treatment with the microtome. This difference was obtained from the plan photos made at a tablet depth of 3.5 mm of which plane both before and after treatment with the microtome photos were taken (90 photos in total).

Number of Transitions

Each picture used for calculating the number of transitions (N_T) was a square image of 1676 × 1676 pixels. A Gaussian filter (σ = 4 pixels) was applied to suppress noise and surface artefacts caused by the microtome before making the images binary with the isodata threshold algorithm. Both these operations were carried out with the DIPimage toolbox. After this step the number of transitions from the salt phase to the pore phase and *vice versa* was calculated. This was done along each pixel line, meaning that for each photo the number of transitions along 3352 lines was counted; in the plan photos this was done along each pixel line in the x-direction and in the y-direction, and in the elevation photos this was done in the z-direction and in the x-direction. Counting the number of transitions is similar to the "line intercept count," a method used in stereology (16) that gives information about the structure of a sample. After calculating the number of transitions, a quotient was calculated by dividing the N_T in one direction by the N_T in the other direction. For the plan photos this meant:

$$Q_P = \frac{N_{Ty}}{N_{Tx}}$$

And for the elevation photos:

$$Q_E = \frac{N_{Tz}}{N_{Tx}}$$

In which:

$Q_{[P,E]}$ = quotient of transitions in [Plan, Elevation] image(s)

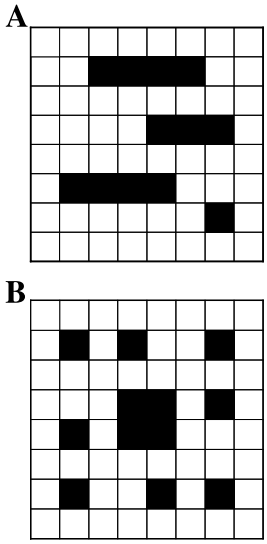

Fig. 3. (A) Square divided in 8 × 8 blocks. Percentage black is 19% and has a preferential direction. (B) Square divided into 8 × 8 blocks. Percentage black is 19% and there is no preferential direction for the black squares.

N_{Ty} = number of transitions in the y-direction
N_{Tx} = number of transitions in the x-direction
N_{Tz} = number of transitions in the z-direction

The method is illustrated in Fig. 3. In both pictures the total number of squares is 8 × 8 = 64. Both pictures have 12 black squares. If the black squares represent the pore phase and the white squares represent the salt phase, the local porosity is in each case 18.8%. However, the quotient of the number of transitions, counted from left to right and from top to bottom, is different for the two pictures: the number of transitions for the picture in Fig. 3A is 8 counted from left to right and 24 counted from top to bottom. This gives a quotient of 0.33. For the picture in Fig. 3B, the quotient is 20/20 = 1. This means that the distribution of black squares is different for the two pictures. It can also be seen that when the quotient deviates from 1, the sample shows anisotropy.

RESULTS AND DISCUSSION

Experimental Procedure

The chemical formula of glycol methacrylate makes it very unlikely that sodium chloride dissolves in this embedding medium. That the particles do not dissolve is also suggested by the still sharp edges of the sodium chloride particles seen in the SEM images. If dissolution had taken place, smooth edges would have been observed as sharp corners dissolve first. After embedding, tablet dimensions stayed the same, also supporting the assumption that the structure is preserved during embedding.

Photos: Visual Observation

Figure 4A is an example of a plan photo. There is a good distinction between the salt particles and the spaces where the polymer is present (pores). The observed shape of the particles is mainly rectangular. Some particles lie separate while others are connected to each other. There does not seem to be a preferential direction of either the pores or the particles. Figure 4B shows an elevation photo. Again there is a clear distinction between the salt-phase and the pore-phase and, just as in the plan photo, the particle's shape is mainly rectangular. However, a difference in structure is discernable. Contrary to the structure in the plan photos, there does seem to be a preferential direction in the elevation photos. Here the particles seem to be connected to each other mainly in the z-direction. However, it is clear that just from the observation the anisotropy is not quantified. Figure 4A and B are both photos taken from the upper surface of the tablets. Photos taken at the different tablet depths show similar structures.

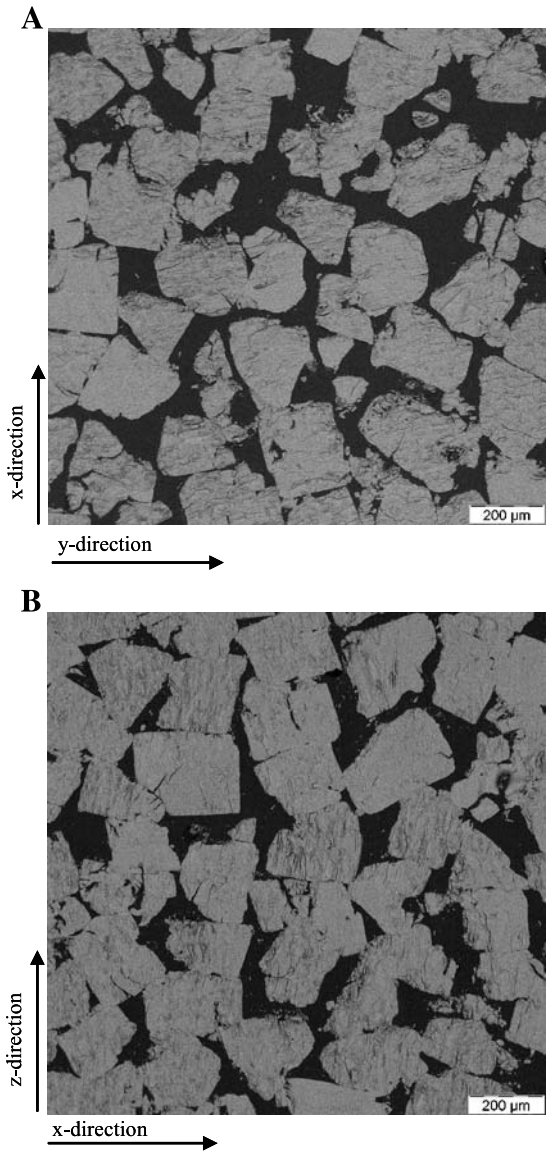

Fig. 4. (A) Plan photo of the upper surface. (B) Elevation photo of the upper surface.

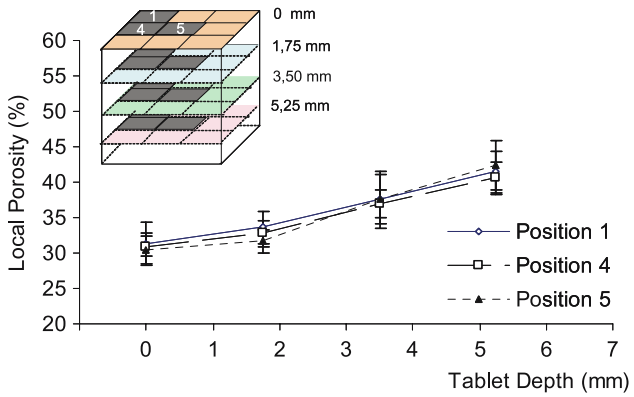

Fig. 5. Surface porosity of the plan photos. Points are the averages of five measurements; error bars are standard deviations. Insert shows photo positions of which the results are shown.

Local Porosity: Plan

Figure 5 shows the local porosities for photo positions 1, 4, and 5. These graphs are representative for the other photo positions. There are hardly differences between the local porosities at the different photo positions. However, differences between the local porosities at different compact depths, compact depth being the distance to the top surface measured in the direction of compression, are considerable. The local porosity increases with increasing compact depth.

The increase in local porosity with increasing compact depth is caused by the fact that the applied compaction pressure is not fully transmitted to lower regions, due to friction between salt particles and the die wall and between the particles themselves (17). This implies that for uniaxial compression, with a stationary lower punch, a density gradient can be found with a higher density at the top of the compact and a lower density in the bottom. Several authors have reported this (17–20), but this effect has not been visualized so far. Another observation that can be made is that the pattern of increasing local porosity with increasing compact depth is similar for all photo positions. This is in contradiction with results of other authors who found higher densities in the top corners compared to the centre of the top layer (17,18,21). The discrepancy is probably caused by the use of different materials. Train used magnesium carbonate (18), Briscoe *et al.* used an alumina powder (21) and Ozkan *et al.* used alumina agglomerates (17). These materials have different properties compared to the sodium chloride used in this study. The use of a different shape of punch and die, and low compression force, can also be the cause of the deviations from previous reported results.

Local Porosity: Elevation

Figure 6 shows mean local porosities and standard deviations of the elevation photos. This is shown for the plane in the middle of the compact at 3.5 mm from the side, but the results are representative for the other planes. The line marked "side A" represents the local porosities of the photo positions 1, 2, and 3. The line "centre" is the result of the measurements from photo positions 4, 5, and 6 and the line "side B" is calculated with positions 7, 8, and 9. The compact depth is the mean tablet depth of the corresponding photos. At all planes the local porosities in the tablet columns side A and side B are not different from the local porosity in the tablet column center.

Contrary to the plan photos, there does not seem to be a relationship between local porosity and compact depth in the elevation photos. This is probably because the compacts are made with uniaxial compression. Because the direction of compression is the z-direction, voids between particles perpendicular to this direction are closed first during compression. It can be argued that pores parallel to the z-direction remain open at this compression force. In the elevation photos these pores are the main pores in the images (see, e.g., Fig. 4B). Apparently the pores in the z-direction exist over the whole tablet depth, explaining the lack of

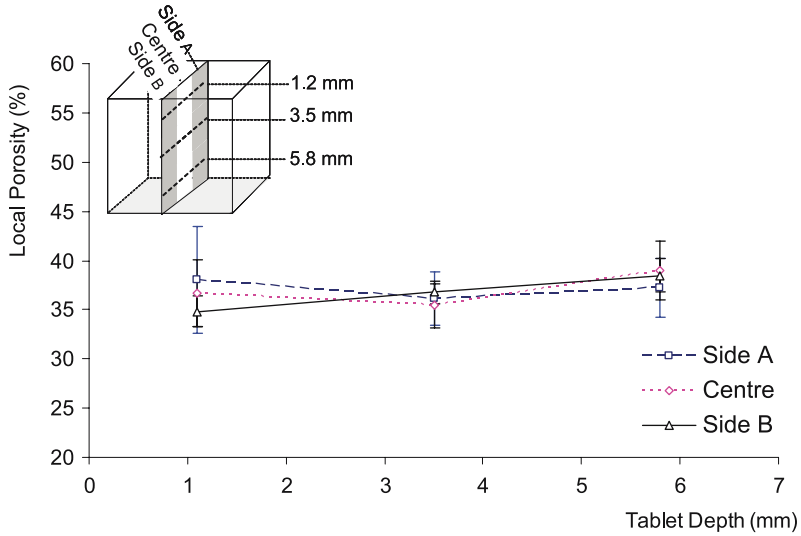

Fig. 6. Surface porosity at different tablet depths for the elevation photos at 3.5 mm from the side. Points represent the averages of five measurements; error bars are standard deviations. Insert shows photo positions of which the results are shown.

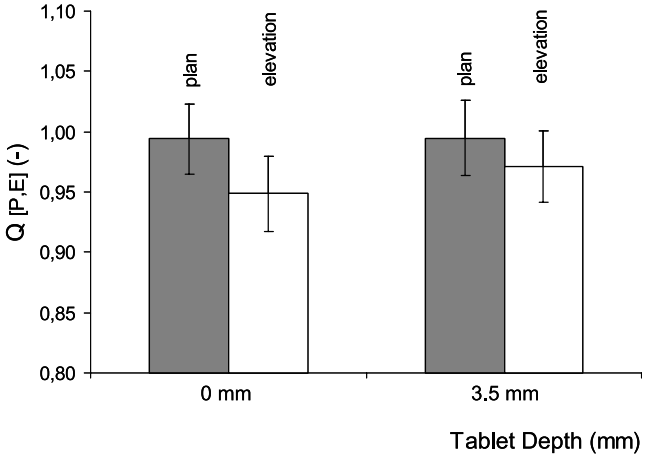

Fig. 7. Quotient of transitions in plan and elevation images.

porosity gradient with increasing tablet depth in the elevation photos.

Both plan and elevation photos show no difference in local porosity between corner positions or the more central parts of the compacts.

Anisotropy

The quotient of transitions, $Q_{[P,E]}$ (see earlier) has been the basis to quantify the preferential direction of the pores in the tablets. Fig. 7 shows the mean values and standard deviations for the plan and elevation planes at 0 mm and 3.5 mm tablet depth. The quotient of transitions in the plan photos does not significantly differ from "unity" in both tablet locations, meaning that there is no preferential direction of the pores in either the x-direction or y-direction. This is in agreement with the image shown in Fig. 4A. However, in the elevation photos, the quotient of transitions is significantly lower than unity (one sample t-test, $p < 0.001$). This implies that the number of transitions in the z-direction is lower than the number of transitions in the x-direction. Hence the pores and particle clusters are preferentially oriented in the z-direction. Particles are pressed together in this direction and it is therefore not surprising that the particles are mainly connected to each other in the z-direction.

Another approach to the same topic is a comparison of the plan photos with the elevation photos. For the upper surface the data show that the quotient number of transitions in the plan photos is significantly higher than in the elevation photos (two-tailed Student's t-test, $p < 0.001$). The same applies to the elevation and plan photos of the planes at 3.5 mm from the tablet surface. This means that the pore distribution as shown in the plan photos is different from the pore distribution as shown in the elevation photos, again proving anisotropy in pore distribution.

CONCLUSION

The method presented in this article is suitable for visualization and quantitative analysis of the pore distribution in tablets. By embedding a cubic sodium chloride compact with polymer it was possible to cut the tablets and make images of the inner structure. These images had a high resolution which made it possible to do a quantitative analysis. This analysis clearly showed a porosity gradient in the tablet with higher porosities toward the underside of the compact. In the elevation photos such a gradient was not found. Still, elevation photos proved their use, since those photos in combination with plan photos clearly showed anisotropy in the tablet structure. In addition, it could be determined that the preferential direction of the pores was the z-direction.

In this study sodium chloride was used as an excipient to introduce the method. The choice for this material showed that the density distributions in a compact as found by other authors (17,18,21) are not universally applicable.

Finally, the method described here seems to be feasible for pore characterization in standard shaped tablets in order to investigate production problems such as lamination and capping.

REFERENCES

1. W. H. Duckworth. Discussion of Ryshkewitch paper by Winston Duckworth. *J. Am. Ceram. Soc.* **36**:68 (1953).
2. B. Van Veen, K. Van der Voort Maarschalk, G. K. Bolhuis, M. Gons, K. Zuurman, and H. W. Frijlink. The influence of particles of a minor component on the matrix strength of sodium chloride. *Eur. J. Pharm. Sci.* **16**:229–235 (2002).
3. A. M. Juppo. Relationship between breaking force and pore structure of lactose, glucose and mannitol tablets. *Int. J. Pharm.* **127**:95–102 (1995).
4. T. Ando, H. Yuasa, Y. Kanaya, and K. Asahina. Studies on anisotropy of compressed powder. III. Effects of different granulation methods on anisotropy, pore size and crushing strength of tablets. *Chem. Pharm. Bull.* **31**:2045–2054 (1983).
5. S. Malamataris, T. Hatjichristos, and J. E. Rees. Apparent compressive elastic modulus and strengths isotropy of compacts formed from binary powder mixes. *Int. J. Pharm.* **141**:101–108 (1996).
6. G. Alderborn and C. Nystrom. Radial and axial tensile strength and strength variability of paracetamol tablets. *Acta Pharm. Suec.* **2**:1–8 (1984).
7. J. M. Newton, G. Alderborn, and C. Nystrom. A method of evaluating the mechanical characteristics of powders from the determination of the strength of compacts. *Powder Technol.* **72**:97–99 (1992).
8. A. M. Bouwman, M. J. Henstra, D. Westerman, J. T. Chung, Z. Zhang, A. Ingram, J. P. K. Seville, and H. W. Frijlink. The effect of the amount of binder liquid on the granulation mechanisms and structure of microcrystalline cellulose granules prepared by high shear granulation. *Int. J. Pharm.* **290**:129–136 (2005).
9. L. Farber, G. Tardos, and J. N. Michaels. Use of X-ray tomography to study the porosity and morphology of granules. *Powder Technol.* **132**:57–63 (2003).
10. A. M. Juppo. Porosity parameters of lactose, glucose and mannitol tablets obtained by mercury porosimetry. *Int. J. Pharm.* **129**:1–12 (1996).
11. B. van Veen, K. van der Voort Maarschalk, G. K. Bolhuis, M. R. Visser, K. Zuurman, and H. W. Frijlink. Pore formation in tablets compressed from binary mixtures as a result of deformation and relaxation of particles. *Eur. J. Pharm. Sci.* **15**:171–177 (2002).
12. H. Vromans, A. H. De Boer, G. K. Bolhuis, C. F. Lerk, K. D. Kussendrager, and H. Bosch. Studies on tableting properties of lactose. Part 2. Consolidation and compaction of different types of crystalline lactose. *Pharm. Weekbl., Sci.* **7**:186–193 (1985).
13. P. Sriamornsak and N. Thirawong. Use of back-scattered electron imaging as a tool for examining matrix structure of calcium pectinate. *Int. J. Pharm.* **267**:151–156 (2003).
14. http://www.ph.tn.tudelft.nl/DIPlib (accessed 3/23/04).

15. T. W. Ridler and S. Calvard. Picture thresholding using an iterative selection method. *IEEE Trans. Syst. Man Cybern.* **8**:630–632 (1978).
16. J. C. Russ and R. T. Dehoff. *Practical Stereology*, Kluwer Academic/Plenum, New York, 2000, pp. 56–61.
17. N. Ozkan and B. J. Briscoe. Characterization of die-pressed green compacts. *J. Eur. Ceram. Soc.* **17**:697–711 (1997).
18. D. Train. An investigation into the compaction of powders. *J. Pharm. Pharmacol.* **8**:745–761 (1956).
19. J. Nam, W. Li, and J. L. Lanutti. Density gradients and springback: environmental influences. *Powder Technol.* **133**: 23–32 (2003).
20. I. C. Sinka, S. F. Burch, J. H. Tweed, and J. C. Cunningham. Measurement of density variations in talbes using X-ray computed tomagraphy. *Int. J. Pharm.* **271**:215–224 (2004).
21. B. J. Briscoe and S. K. Sinha. Density distributions characteristics of green ceramic compacts using scratch hardness. *Tribol. Int.* **30**:475–482 (1997).